

Ultraviolet photoelectron spectroscopy of the phenide, benzyl and phenoxide anions, with ab initio calculations*

Robert F. Gunion^{a,b}, Mary K. Gilles^{a,b}, Mark L. Polak^{a,b} and W.C. Lineberger^{a,b}

^aJoint Institute for Laboratory Astrophysics, National Institute of Standards and Technology University of Colorado and ^bDepartment of Chemistry and Biochemistry, University of Colorado, Boulder CO 80309-0440 (USA)

(First received 14 February 1992)

ABSTRACT

The 351 nm photoelectron spectra of the phenide, benzyl and phenoxide anions are reported. Information obtained for phenyl radical includes an adiabatic electron affinity (EA) of 1.096(6) eV, two vibrational modes at 600(10) and 968(15) cm⁻¹, and an excited electronic state at ≤ 1.7 eV. For benzyl, the radical EA is 0.912(6) eV, a vibration appears at 514(15) cm⁻¹, and another is possibly present at 1510(25) cm⁻¹. Phenoxyl radical has an EA of 2.253(6) eV, exhibits a vibration at 515(15) cm⁻¹, and possibly another at 1490(25) cm⁻¹. The first excited state of phenoxyl radical appears at 1.06(5) eV above the ground state. Ab initio calculations using GAUSSIAN 88 are used to elicit geometries, normal modes of the active vibrations, and help confirm the presence of various vibrations. Combining our results with previous measurements we find gas-phase acidities for benzene and toluene of 399(2) kcal mol⁻¹ and 380.5(1.5) kcal mol⁻¹ respectively, and a hydrogen bond dissociation energy for phenol of 86.5(2) kcal mol⁻¹.

Keywords: ab initio calculations; benzyl anion; phenide anion; phenoxide anion; UV photoelectron spectroscopy.

INTRODUCTION

Ultraviolet photoelectron spectroscopy has been extremely useful in studying many molecules ranging from small organic molecules to metal clusters [1]. The determination of extremely accurate adiabatic electron affinities is trivial in most molecules, and electronic and vibrational state energies unavailable to optical spectroscopy because of selection rules can often be determined in both anions and the corresponding neutrals. This method has even proven to be a sensitive probe of the rearrangement of unstable radicals, such as the migration of a hydrogen in vinylidene to form

Correspondence to: W.C. Lineberger, Joint Institute for Laboratory Astrophysics, Department of Chemistry, University of Colorado, Boulder CO 80309-0215, USA.

*Dedicated to Professor Charles H. DePuy on the occasion of his 65th birthday.

acetylene [2] and a similar recent investigation [3] of $\text{C}=\text{CHF}$. *Ortho*-benzynes (C_6H_4^-) [4] is the only small organic ring system which has been studied using photoelectron spectroscopy to date, so the molecules investigated here represent the first excursion of photoelectron spectroscopy into small fully aromatic ring systems. As such, the degree of detail obtained from the spectra is necessarily less than for smaller systems.

Over the past several years advances in computing speed and the availability of sophisticated *ab initio* calculation programs have made possible their almost routine use as supplements to experimental work. Specifically, the GAUSSIAN 88 [5] program allows experimentalists to perform elaborate calculations on large molecules. For this reason, we were able to obtain geometry and frequency calculations on all three of the radicals and anions in this work at a higher level of theory than has been employed previously. These calculations help immensely in the interpretation of the photoelectron spectra of such large molecules.

The phenide (C_6H_5^-), benzyl ($\text{C}_6\text{H}_5\text{CH}_2^-$), and phenoxide ($\text{C}_6\text{H}_5\text{O}^-$) anions provide a comprehensive test of electron detachment from aromatic systems. Phenide anion is the conjugate base of benzene, making the neutral a prototype of aromatic radicals; however, interesting changes in the phenyl electron density may occur as a result of the presence of a radical center rather than a carbon–hydrogen bond. The benzyl and phenoxide anions are isoelectronic, except that benzyl has two hydrogen atoms where phenoxide has two oxygen lone pairs. The $-\text{CH}_2$ group on benzyl is only weakly electron withdrawing while the phenoxyl oxygen atom is strongly electron withdrawing. This gives us a range of substituent effects between the three radicals for investigating the behavior of phenyl rings in a wide range of compounds.

Data on the phenyl, benzyl and phenoxyl radicals relevant to this work have been reported independently by several authors, including Professor Charles H. DePuy, to whom this issue is dedicated. DePuy et al. [6] measured the gas phase acidity of benzene as $399 \pm 2 \text{ kcal mol}^{-1}$; using this with McMillen and Golden's [7] bond dissociation energy (BDE) of $111 \pm 2 \text{ kcal mol}^{-1}$ they arrived at a phenyl radical electron affinity (EA) of $1.1 \pm 0.1 \text{ eV}$. The gas phase acidity measurement was confirmed by Meot-Ner and Sieck [8] in a variable temperature high pressure mass spectrometer ($\Delta H_{\text{acid}}(\text{C}_6\text{H}_6) = 400.8 \pm 2.5 \text{ kcal mol}^{-1}$ at 600 K), from which they arrived at an electron affinity of phenyl radical of $1.0 \pm 0.1 \text{ eV}$. Phenyl radical ($^2\text{A}_1$ ground state) [9,10] has been observed in matrices by Pacansky and Bargon [11] and by Jacox [12]. Dewar et al. [13] performed a CNDO calculation on the phenyl radical to arrive at a heat of formation of 73 kcal mol^{-1} and to find the vibrational modes available to the phenyl radical, though no symmetries were assigned to these vibrations.

The planar geometry of the benzyl radical was calculated (STO-3G level)

by Vanermen et al. [14] to be 26 kJ mol^{-1} more stable than the tetrahedral configuration around the benzylic carbon atom. Spectra of the benzyl radical have been obtained in matrices [15–17] and in the gas phase [18,19]. For some time the symmetry of the first excited state was unknown, until Cossart-Magos and Leach [18] extracted its identity as 2A_2 from gas phase emission spectra; they subsequently investigated the vibronic coupling between this state and a 2B_2 electronic state only $430\text{--}485 \text{ cm}^{-1}$ above it [19]. Drzaic and Brauman [20] reported the electron affinity of benzyl radical as $0.86 \pm 0.01 \text{ eV}$, using ion cyclotron resonance (ICR) laser photodetachment spectroscopy. Calculations on the orbital configuration of benzyl radical have been done at the configuration interaction (CI) level [21] using bond angles equal to 120° , bond lengths of 1.4 \AA and an electron affinity of 0.03 eV . The optical absorption spectra of benzyl and phenoxyl radicals were obtained by Ward [22]. Raman spectra of phenoxyl in water exhibited vibrations of the radical at 548, 960, 1518, 1558 cm^{-1} and higher [23]. McMillen and Golden [7] reported the bond dissociation energies of $C_6H_5\text{--}H$ ($110.9 \pm 2 \text{ kcal mol}^{-1}$), $C_6H_5O\text{--}H$ ($86.5 \pm 2 \text{ kcal mol}^{-1}$) and $C_6H_5CH_2\text{--}H$ ($87.9 \pm 1.5 \text{ kcal mol}^{-1}$) in a review article.

In this study we present the photoelectron spectra of the phenide, benzyl and phenoxide anions. First we briefly describe the experimental techniques used to obtain the photoelectron spectra, then present the results, including electron affinities, vibrational frequencies, and photoelectron angular distribution measurements. The results section concludes with a description of Hartree–Fock calculations for each of the radicals and anions. The Analysis and Discussion section describes the procedure used to analyze the spectra, and the vibrational modes of the three radicals are identified. The effects of the aromatic ring on electron affinities are examined. The photoelectron angular distributions are discussed, and finally a simple thermochemical cycle is used to determine bond strengths and gas phase acidities.

EXPERIMENT AND RESULTS

The UV photoelectron spectrometer used in this work has been described in detail elsewhere [1] so only a brief description will be given here. The ions are produced using controlled thermal ion chemistry in a flowing afterglow ion source [24]. A buffer gas consisting of $400\text{--}800 \text{ mTorr}$ helium and trace amounts of oxygen or NF_3 is passed through a microwave discharge, then allowed to react with small concentrations of a precursor, from which the desired negative ions are formed. The ions are extracted into a differentially pumped region, accelerated, focused into a Wien velocity filter (resolution $m/\Delta m$ 40), and finally decelerated before entering the laser interaction region. In this region the electrons are photodetached by laser light at 3.531 eV and

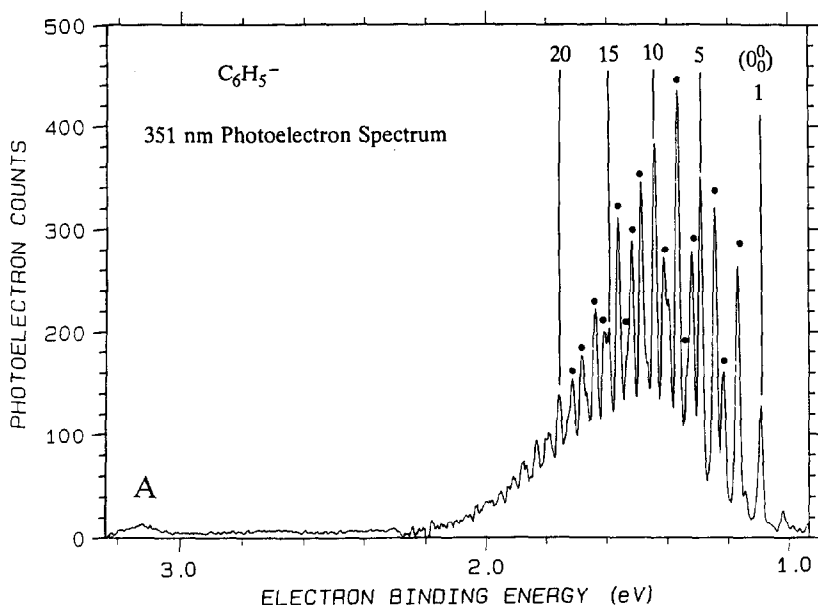


Fig. 1. Photoelectron spectrum of phenide anion (351 nm photon energy). Peak marked "A" is an excited electronic state of phenyl radical. Numbered peaks are those included in Table 1.

their kinetic energies measured in a hemispherical electrostatic energy analyzer (resolution 8–10 meV) [25].

The C_6H_5^- ion is formed in the flowing afterglow source using benzene as the precursor and F^- (from NF_3) in the helium buffer. The $\text{C}_6\text{H}_6 + \text{F}^- \rightarrow \text{C}_6\text{H}_5^- + \text{HF}$ reaction itself is 79 kcal mol^{-1} endothermic [26], so the mechanism by which this reaction proceeds is not straightforward; however, ion currents of 50–100 pA are obtainable. *Ortho*-benzyne (C_6H_4^-) also forms in this reaction and our mass filter cannot completely separate it from the phenide anion. Since the photoelectron spectra of C_6H_4^- and C_6H_5^- overlap, benzyne is a contaminant of the phenide spectrum. The C_6D_5^- spectrum exhibits no such contamination, confirming the identity of the phenide ion. To eliminate any benzyne contamination from the phenide spectrum, a more benzyne-rich spectrum has been subtracted from the phenide spectrum shown in Fig. 1. Judging from the relative peak intensities and positions of the unsubtracted spectrum and *ortho*-benzyne spectra studied in this laboratory [4] we are confident that the only significant C_6H_4^- contamination is in the region of the phenide anion hot bands (less than 1.0 eV electron binding energy); this contamination precludes our determining vibrational frequencies of the phenide anion.

An excited state of the phenyl radical appears at high electron binding energies (peak "A" in Fig. 1). The signal level is too low to resolve any

TABLE 1

Phenyl spectrum assignments

Peak no.	Distance from origin (cm ⁻¹)		Assignment ($\nu_1 = 600\text{ cm}^{-1}$; $\nu_2 = 968\text{ cm}^{-1}$)	Peak height (counts)	
	Observed	HO est. ^a		Observed	Franck–Condon fit
1	0	0	0 ₀ ⁰	130	120
2	600	600	1 ₀ ¹	250	310
3	980	968	2 ₀ ¹	160	130
4	1200	1200	1 ₀ ²	330	400
5	1570	1568	1 ₀ 2 ₀ ¹	360	340
6	1810	1800	1 ₀ ³	280	350
7	1980	1936	2 ₀ ²	160	70
8	2165	2168	1 ₀ 2 ₀ ¹	440	440
9	2520	2536	1 ₀ 2 ₀ ²	280	180
10	2765	2768	1 ₀ 2 ₀ ³	380	380
11	3130	3136	1 ₀ 2 ₀ ²	350	240
12	3370	3368	1 ₀ 2 ₀ ¹	290	250
13	3535	3504	1 ₀ 2 ₀ ³	170	70
14	3735	3736	1 ₀ 2 ₀ ²	320	210
15	3990	3968	1 ₀ 2 ₀ ¹	200	130
16	4105	4104	1 ₀ 2 ₀ ³	200	90
17	4330	4336	1 ₀ 2 ₀ ²	210	130
18	4685	4704	1 ₀ 2 ₀ ³	180	70
19	4930	4936	1 ₀ 2 ₀ ²	160	70
20	5320	5304	1 ₀ 2 ₀ ³	140	50

^aPeak positions determined by independent harmonic oscillator (HO) approximation.

vibrational structure, but subtracting the electron affinity from the vertical binding energy of this excited state peak yields an upper limit of 1.7 eV for the excitation energy.

The C₆H₅⁻ spectrum is possibly the most complex negative ion photoelectron spectrum that contains detailed structure observed to date. The origin (0₀⁰) is unambiguous, however, giving an EA of 1.096(6) eV, in excellent agreement with the 1.1 eV predicted by bracketing experiments of DePuy et al. [6]. From the peak positions listed in Table 1, we find two vibrational progressions at 600(10) and 968(15) cm⁻¹ (588(10) and 960(20) cm⁻¹ for C₆D₅⁻). However, unusual intensities of peaks and a highly extended, complicated progression make the extraction of more detailed information difficult and we leave further interpretation of the phenide spectrum to the Analysis and Discussion section.

The benzyl anion, C₆H₅CH₂⁻, is formed in a similar fashion to C₆H₅⁻, using O⁻ (from O₂ upstream) rather than F⁻, and toluene in place of benzene. The

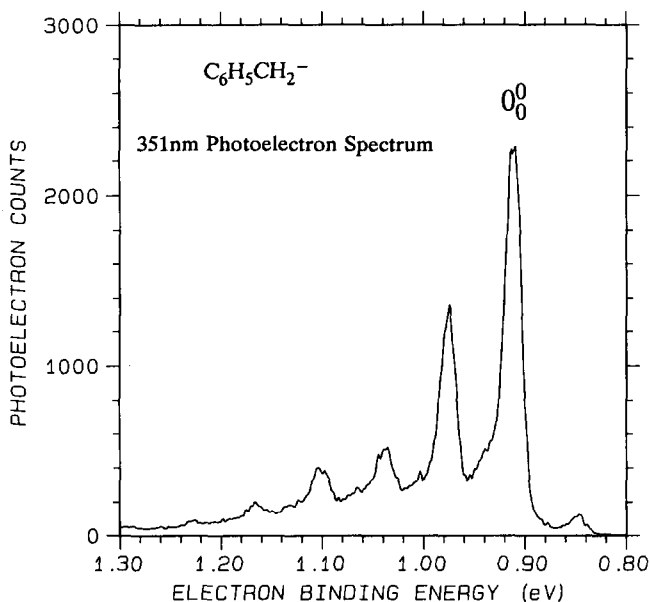


Fig. 2. Photoelectron spectrum of benzyl anion (351 nm).

mass spectrum shows no significant peaks or shoulders near the benzyl peak, and the photoelectron spectrum shows no contamination from other substances. The $\text{C}_6\text{H}_5\text{CH}_2^-$ spectrum, taken with an ion current of 45 pA, is shown in Fig. 2. The adiabatic electron affinity (0.912(6) eV) and a vibrational progression of $514(15)\text{cm}^{-1}$ are immediately apparent. Only the ground electronic state of the radical is accessible by our laser at 3.531 eV, which is consistent with observations of the $^2\text{A}_2$ first excited state at 2.73 eV above the ground state [28].

The phenoxide anion, $\text{C}_6\text{H}_5\text{O}^-$, is formed by the reaction of benzene and O^- in the reaction $\text{C}_6\text{H}_6 + \text{O}^- \rightarrow \text{C}_6\text{H}_5\text{O}^- + \text{H}$. The enthalpy change of this reaction is -34 kcal mol^{-1} [26]. Typical ion currents of phenoxide are around 45 pA. Some contamination was present from a molecule at slightly higher mass than phenoxide, but by adjusting the mass filter while taking photoelectron spectra we were able to confirm that the spectra in Figs. 3 and 4 are purely due to phenoxide.

Although the EA of phenoxyl is 1.3 eV greater than that of benzyl, the phenoxide spectrum is very similar to that of benzyl. The electron affinity is clearly determined from the position of the origin peak as 2.253(6) eV, and a single vibrational mode is clearly present at $515(15)\text{cm}^{-1}$. The first excited electronic state of the phenoxyl radical is present at high electron binding energy and marked "A" in Fig. 3; using the maximum of this peak we estimate the position of the state to be 1.06(5) eV above the ground state. The lowest

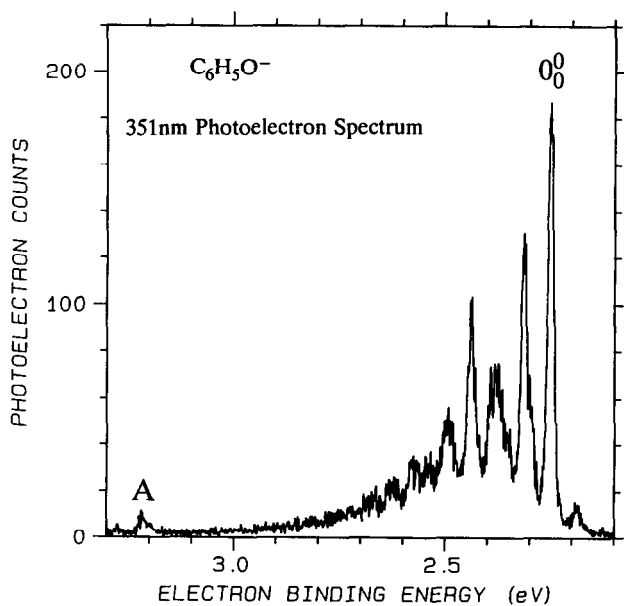


Fig. 3. Photoelectron spectrum of phenoxide anion (351 nm). Peak marked "A" is an excited electronic state of phenoxyl radical.

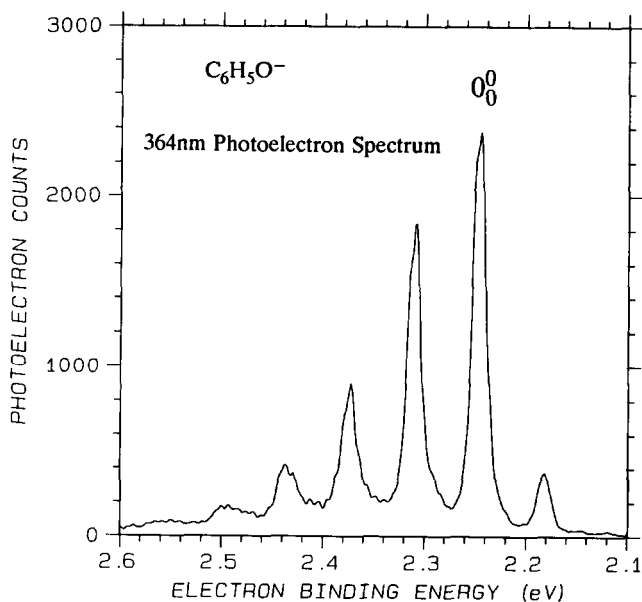


Fig. 4. Photoelectron spectrum of phenoxide anion (364 nm).

TABLE 2

Experimentally determined values from this work

A	Adiabatic electron affinity (eV)	First excitation energy (eV)	Asymmetry parameter β (0% peak)	$\Delta H_{\text{acid}}(\text{AH})$ (kcal mol ⁻¹) ^a	BDE(AH) (kcal mol ⁻¹)
Phenyl	1.096(6)	≤ 1.7	0.15	[400.8(2.5)] [8]	112.6(2.5)
Benzyl	0.912(6)		-0.42	380.5(1.5)	[87.9(1.5)] [36]
Phenoxy	2.253(6)	1.06(5)	-0.53	[348.5(2)] [39]	86.5(2)

^a Values in brackets are from the literature.

previously observed state is 2.03 eV above the ground state [27]. We would intuitively expect the lowest excited state of phenoxy to have $^2\text{B}_1$ symmetry, and the existence of such a state was suggested [28] to lie 0.53 eV above the ground state by a CNDO calculation, indicating that the state we observe may be this $^2\text{B}_1$ state.

The spectrum in Fig. 3 was obtained with our normal photon energy, 3.531 eV. It does not follow a simple Franck–Condon progression and several unidentified peaks appear, indicating that autoionization of the anion may be an interference in the photoelectron signal. This is confirmed by reducing the photon energy to 3.408 eV (Fig. 4): the peaks form a simpler Franck–Condon progression and the unidentified peaks disappear. The differences between these spectra imply that phenoxide anion has a metastable state approximately 3.5 eV above its ground state; since 3.408 eV photons appear not to access the metastable state, the 3.408 eV spectrum is much simpler. Therefore Franck–Condon fits were carried out using the 3.408 eV spectrum.

All the spectra presented in Figs. 1–4 were taken at the “magic angle” (54.7°) of laser polarization to photoelectron collection. The spectrum of each molecule was also taken at the parallel ($\theta = 0^\circ$) and perpendicular ($\theta = 90^\circ$) polarizations by rotating a half-wave plate. Expressions derived by Cooper and Zare [29] allow us to estimate the asymmetry parameter β for photodetached electrons using the equation

$$\beta = \frac{I_0 - I_{90}}{(1/2)I_0 + I_{90}} \quad (1)$$

where I_0 is the intensity of a given peak in the parallel photoelectron detachment spectrum and I_{90} is the intensity for perpendicular detachment. In Table 2 we report the asymmetry parameter for the origin peak of each spectrum; it is nearly constant for all peaks in the benzyl and phenoxide spectra, but varies between 0.15 and 0.30 in the phenide spectrum.

In addition to experimental data, ab initio calculations were performed on

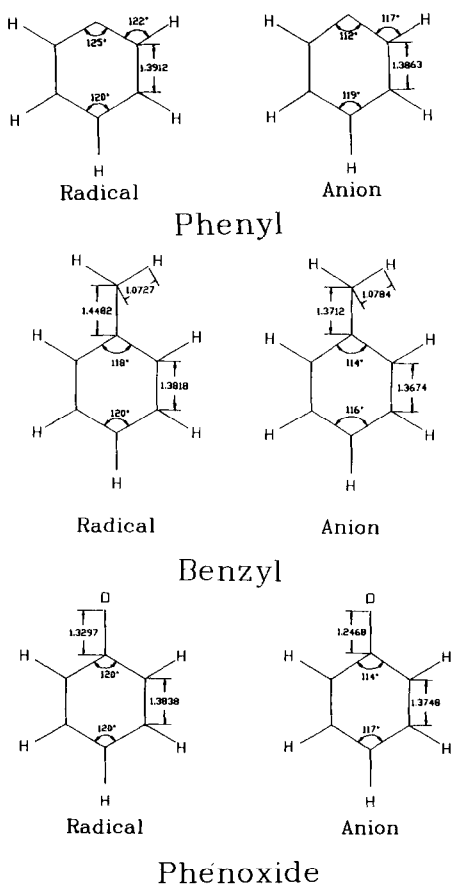


Fig. 5. Ab initio geometries of all anions and radicals (HF/6-31G** level). Selected bond lengths are indicated in Ångströms, and bond angles in degrees.

each of the anions and radicals using GAUSSIAN 88; Fig. 5 shows the optimized geometries including selected bond lengths and angles. The machines used were an IBM RS6000-540 and an IBM RS6000-550, each running under AIX v. 3.1. Anion geometry calculations used restricted Hartree–Fock methods, while restricted open-shell Hartree–Fock methods were used for the radicals. First crude geometries were obtained with small basis sets, then a 6-31G** basis set was used to arrive at final converged geometries. All geometries were constrained to C_{2v} symmetry. Ground electronic state vibrational frequencies, listed in Table 3, were calculated for each species using the geometries provided by the 6-31G** basis set calculations. Since vibrational frequencies calculated using Hartree–Fock methods are typically 10% higher than experimental frequencies, the values reported in Table 3 have been scaled from those calculated accordingly.

TABLE 3

Frequencies of all modes determined by HF/6-31G**//6-31G** calculations, scaled to 90% of those actually calculated^a

Mode no.	Phenyl		Benzyl		Phenoxy	
	Radical	Anion	Radical	Anion	Radical	Anion
1	405 (A2)	379 (A2)	211 (A1)	171 (B1)	232 (B1)	202 (B1)
2	423 (B1)	399 (B1)	303 (A2)	345 (B2)	394 (A2)	424 (A2)
3	587 (B2)	582 (A1)	339 (B2)	417 (A2)	407 (B2)	434 (B2)
4	596 (A1)*	608 (B2)	413 (A2)	439 (B1)	492 (B1)	501 (B1)
5	671 (B1)	676 (B1)	420 (B1)	482 (B1)	513 (A1)*	514 (A1)
6	723 (B1)	714 (B1)	495 (B1)	506 (A1)	516 (B2)	596 (B2)
7	843 (A2)	843 (B1)	514 (A1)*	565 (A2)	681 (B1)	688 (B1)
8	902 (B1)	862 (A2)	612 (B2)	604 (B2)	684 (B1)	703 (B1)
9	965 (A1)*	933 (A1)	693 (B1)	615 (B1)	813 (A1)	796 (A2)
10	980 (A1)*	960 (A2)	758 (B1)	693 (B1)	853 (A2)	800 (A1)
11	985 (A2)	964 (B1)	791 (A1)	777 (A1)	954 (B1)	838 (B1)
12	1007 (B1)	969 (A1)	853 (A2)	779 (A2)	983 (A1)	943 (A1)
13	1017 (A1)	1016 (B2)	920 (B1)	787 (B1)	997 (A2)	954 (B1)
14	1031 (B2)	1016 (A1)	946 (B2)	927 (B2)	1004 (A1)	956 (A2)
15	1093 (B2)	1079 (B2)	975 (A1)	937 (A1)	1017 (B1)	990 (A1)
16	1145 (A1)	1150 (B2)	986 (A2)	949 (B1)	1049 (B2)	1035 (B2)
17	1204 (B2)	1151 (A1)	1008 (B1)	953 (A2)	1092 (B2)	1101 (B2)
18	1281 (B2)	1296 (B2)	1014 (A1)	986 (A1)	1131 (A1)	1132 (A1)
19	1429 (B2)	1403 (B2)	1064 (B2)	1059 (B2)	1190 (A1)	1164 (B2)
20	1462 (A1)	1425 (A1)	1098 (B2)	1115 (B2)	1200 (B2)	1293 (B2)
21	1578 (A1)	1543 (B2)	1161 (A1)	1151 (A1)	1297 (B2)	1383 (A1)
22	1609 (B2)	1560 (A1)	1203 (A1)	1229 (B2)	1446 (B2)	1448 (B2)
23	3004 (A1)	2856 (B2)	1205 (B2)	1306 (A1)	1476 (A1)*	1528 (B2)
24	3012 (B2)	2859 (A1)	1325 (B2)	1309 (B2)	1595 (A1)	1547 (A1)
25	3025 (A1)	2910 (A1)	1449 (A1)	1442 (A1)	1601 (B2)	1602 (A1)
26	3032 (B2)	2916 (B2)	1451 (B2)	1449 (B2)	3011 (A1)	2928 (A1)
27	3037 (A1)	2958 (A1)	1491 (A1)*	1504 (B2)	3023 (B2)	2932 (B2)
28			1593 (B2)	1507 (A1)	3032 (A1)	2978 (A1)
29			1614 (A1)	1597 (A1)	3042 (B2)	2979 (B2)
30			2997 (A1)	2921 (A1)	3044 (A1)	2991 (A1)
31			3001 (A1)	2923 (B2)		
32			3004 (B2)	2936 (A1)		
33			3015 (A1)	2961 (B2)		
34			3021 (B2)	2964 (A1)		
35			3033 (A1)	2990 (A1)		
36			3092 (B2)	2995 (B2)		

^a A₁ modes are italic; modes observed in this work are marked with asterisks.

ANALYSIS AND DISCUSSION

Vibrations

Since photodetachment of an electron occurs much more quickly than one period of a vibration, the molecule cannot rearrange significantly while the electron is being ejected. Therefore vibrational peak intensities are determined by the Franck–Condon principle, where intensities are proportional to the overlap of the anion vibrational wavefunctions with those of the neutral. For such overlap to be non-zero, the symmetries of the vibrational states must be the same in the anion initial state and the neutral final state. In the case of the phenide, benzyl and phenoxide anions, which are prepared with vibrational temperatures of 300–400 K, virtually all the initial population is in the ground vibrational state (A_1 symmetry); therefore only A_1 vibrations can be active in the photoelectron spectra for these molecules. For this reason, all A_1 vibrations calculated by GAUSSIAN 88 have been italicized in Table 3 to indicate that they are symmetry allowed for photoelectron spectroscopy.

The A_1 symmetry selection rule provides for 10 possible modes in phenide, 13 in benzyl, and 11 in phenoxide, approximately one-third of the total number of vibrations available to each molecule. The photoelectron spectra would be virtually impossible to analyze if every A_1 mode were active, so despite the complications to be outlined below we are fortunate to find only two clearly active modes in each spectrum. The most remarkable aspect of the spectra in Figs. 1–4 is not their intensity anomalies and other complications, but their relative simplicity considering the sizes of the molecules.

Even with this simplicity, however, assignments of the vibrations in the photoelectron spectra would be extremely difficult without some additional information, which we obtain from the GAUSSIAN 88 calculations. To assess the accuracy of these calculations we compare the predicted frequencies (Table 3) with those determined experimentally in previous work.

(1) Seventeen vibrational frequencies in the gas phase and their symmetries have been determined for the benzyl radical [27]. The scaled GAUSSIAN 88 calculations predict a vibration with the correct symmetry corresponding to each of the experimentally determined vibrations within about 50 cm^{-1} , enabling us to use this as a rough error estimate.

(2) Only one frequency has been observed previously for the phenyl radical [11,12,30] and no symmetry assignment was attempted. This mode (in an argon matrix) is at 707 cm^{-1} for C_6H_5 and at 519 cm^{-1} for C_6D_5 . Our calculations show two C_6H_5 vibrational modes in this region: 671 and 723 cm^{-1} (Table 3); however, only one of these drops to the 500 cm^{-1} range in our C_6D_5 calculations (525 cm^{-1}). It is also worth noting that in both cases

this mode is calculated to be highly IR active. Therefore we can assign this mode as a B_1 out-of-plane CH bend mode.

(3) To our knowledge, no vibrations in the gas phase for the ground state of the phenoxyl radical have been observed. Our assignments here, then, represent new information. Since benzyl is isoelectronic with phenoxide and the spectra of the two anions are very similar, we can use the information obtained from analysis of the benzyl vibrations to assign vibrations in phenoxyl.

By analyzing peak positions in our phenide spectrum (Fig. 1) we find that at least two vibrations are present, at $600(10)$ and $968(15)\text{ cm}^{-1}$. Table 1 lists the first 20 measured peak positions along with the peak positions which would result if the two vibrations were independent harmonic oscillators. The agreement is quite good, and from this we can assign each of the 20 transitions as listed in the third column of Table 1. In the last two columns of Table 1 the experimental and Franck–Condon calculated peak heights are listed; the fit reproduces the peak heights surprisingly well, considering the potential complications in a spectrum of such a large molecule.

We can make some qualitative observations in order to gain some insight into the motion responsible for such a complex spectrum. The ejected electron is somewhat localized around the anionic carbon (C_1), so a CC deformation involving an increase in the $C_6C_1C_2$ angle should be active, and the phenyl radical and anion geometries should be dramatically different from one another. This large change is evident in the geometries obtained from *ab initio* calculations (Fig. 5). As one would expect from VSEPR theory, the lone pair in the anion forces the $C_6C_1C_2$ angle to shrink to 112° , considerably smaller than the CCC bond angle in benzene (120°). However, the single electron in the phenyl radical allows the bond to open up to 125° , inducing a large ring distortion on conversion from the anion to the neutral. Thus the highly extended Franck–Condon profile in the photoelectron spectrum is explained; however, further insight will be needed to understand the spectrum.

For this we need the frequency calculations predicted for A_1 modes by GAUSSIAN 88. The 600 cm^{-1} mode observed in the phenide spectrum has a clear counterpart in the calculations at 596 cm^{-1} ; the normal coordinates predicted by GAUSSIAN 88 are depicted in Fig. 6(a). Unfortunately, the other mode observed in the spectrum (968 cm^{-1}) could be described by any of three predicted vibrations in this frequency range (Table 3: 965 , 980 and 1017 cm^{-1}). Deuterium substitution experiments eliminate one of these possibilities. The C_6D_5 photoelectron spectrum does not show a large change in this mode (to 960 cm^{-1}), while the 1017 cm^{-1} mode in the C_6H_5 calculations changes to 794 cm^{-1} for C_6D_5 . The other two calculated modes, however, do not change much on deuteration (933 cm^{-1} and 944 cm^{-1} respectively), so we still cannot identify the higher frequency mode with absolute certainty. Here lies a

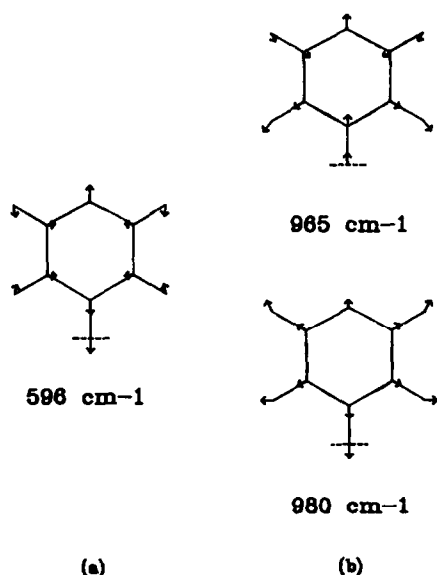


Fig. 6. Calculated normal modes for the possible vibrations observed in the phenide spectrum. When the position of an atom is ambiguous it is indicated with a broken line: (a) mode corresponding to the observed 600 cm^{-1} vibration; (b) two possibilities for the 968 cm^{-1} mode; the data are insufficient to determine which is active.

possible explanation for the complexity of the phenide spectrum; if both of the modes in Fig. 6(b) are active, they could produce many peaks at close frequencies but with different intensity distributions. The normal coordinates of the C_6H_5 modes predicted by GAUSSIAN 88 at 965 and 988 cm^{-1} are presented in Fig. 6(b).

On the surface, the benzyl and the phenoxide spectra (Figs. 2 and 4 respectively) are not only surprisingly simpler than the phenide spectrum, but they are almost identical to one another. For example, each exhibits one very clear vibrational mode at just over 500 cm^{-1} . At first glance the spectra look like a simple progression, with only a small geometry change, in this mode alone. But in each spectrum the third and subsequent peaks from the origin are much too intense for such a simple progression, implying that a second mode may appear at approximately 1500 cm^{-1} . In addition, the spectra do not return to the baseline between peaks; in fact an artificial baseline seems to be present in the region of photodetachment. The peaks are also skewed towards one side, extending to one side much farther than to the other. In a sense the most striking feature of these spectra is their only major difference: the benzyl peaks are skewed towards the high binding energy side but the phenoxide spectrum is skewed in the opposite direction. Thus these two spectra are much

TABLE 4

Peak positions and heights of benzyl and phenoxide transitions

	Distance from origin (cm ⁻¹)		Assignment	Peak height (counts)	
	Observed	HO est. ^a		Observed	Franck–Condon fit
Benzyl	– 514	– 514	1 ₁ ⁰	120	120
	0	0	0 ₀ ⁰	2300	2400
	516	514	1 ₀ ¹	1300	1400
	1025	1028	1 ₀ ²	510	440
	1530	1510	2 ₀ ¹	400	390
		1542	1 ₀ ³		110
	2040	2024	1 ₀ ⁴ 2 ₀ ¹	190	190
		2056	1 ₀ ⁴		24
Phenoxide	– 520	– 515	1 ₁ ⁰	370	250
	0	0	0 ₀ ⁰	2400	2400
	515	515	1 ₀ ¹	1800	1800
	1030	1030	1 ₀ ²	840	750
	1520	1490	2 ₀ ¹	410	300
		1545	1 ₀ ³		200
	2010	2005	1 ₀ ⁴ 2 ₀ ¹	180	200
		2060	1 ₀ ⁴		38

^a Peak positions determined by the independent harmonic oscillator (HO) approximation.

more difficult to understand than they first appear, and again the *ab initio* calculations provide essential guidance.

Peak positions in the benzyl spectrum (Fig. 2), as listed in Table 4, show a dominant vibration at 514 cm⁻¹. Table 3 lists an A₁ vibration at 514 cm⁻¹, so we assign this with confidence and present the normal coordinates from GAUSSIAN 88 in Fig. 7(a). Taking into account the enhanced intensities of the third and subsequent peaks, as well as their slight shift from a simple 514 cm⁻¹ progression, lets us tentatively assign a second vibration at 1510 cm⁻¹. Jacox [27] reports two A₁ vibrations in this region, at 1431 and 1603 cm⁻¹; these bracket the observed 1510 cm⁻¹ mode. But on looking at Table 3 we see that the experimental 1603 cm⁻¹ mode shows up at 1614 cm⁻¹, the 1431 cm⁻¹ vibration is calculated at 1449 cm⁻¹, and another mode lies between them at 1491 cm⁻¹; the normal coordinate for this mode is pictured in Fig. 7(b). This gives strong support for the presence of the 1510 cm⁻¹ mode, as well as the dependability of our *ab initio* calculations, since it corresponds to a mode previously unobserved experimentally but predicted by the calculations. Another factor in support of the activity of this mode is that it involves a C–CH₂ stretch, a motion expected on examination of the anion and radical

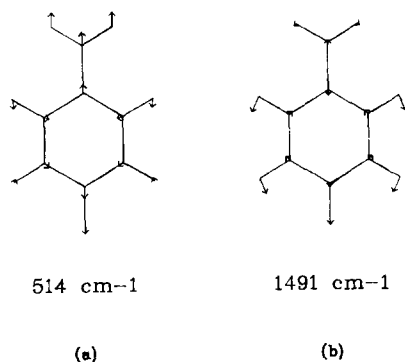


Fig. 7. Calculated normal modes for the vibrations observed in the benzyl spectrum: (a) the 514 cm^{-1} mode; (b) possibly the 1510 cm^{-1} vibration (the photoelectron data are insufficient to determine whether this mode is active).

geometries in Fig. 5. The 514 cm^{-1} mode does not contain such a stretch, so the 1510 cm^{-1} mode is the only apparent channel for motion in this coordinate.

The ground electronic state spectrum of the phenoxyl radical (Fig. 4) shows a vibrational progression in the neutral at $515(15)\text{ cm}^{-1}$ and possibly another at $1490(25)\text{ cm}^{-1}$. The assignment of the second mode cannot be verified by previous experiments, but it is accounted for in the *ab initio* calculations; therefore we tentatively assign our 1490 cm^{-1} mode to one calculated at 1476 cm^{-1} (Table 3). Figure 8 shows the normal coordinates for the 513 and 1476 cm^{-1} modes predicted by GAUSSIAN 88 for the phenoxyl radical; these are exactly analogous to the modes active in the benzyl radical. The 1476 cm^{-1} mode involves a C-O stretch while the 513 cm^{-1} mode does not, indicating that this motion is almost certainly active in the spectrum.

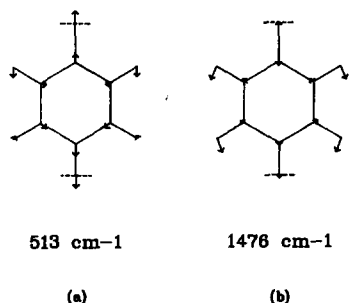


Fig. 8. Calculated normal modes for the vibrations observed in the phenoxide spectrum (when the position of an atom is ambiguous it is indicated with a dotted line): (a) the 515 cm^{-1} mode; (b) possibly the 1490 cm^{-1} vibration (the photoelectron data are insufficient to determine whether this mode is active).

Substituent effects

The trends in the above electron affinities show how the presence of a π aromatic system influences the stabilities of electrons on substituents. The electron affinity of the phenyl radical (1.096 eV) is considerably higher than that of the simplest molecule with an sp^2 hybridized carbon, CH_2 (0.652(6) eV) [24]. Therefore, the ring system contributes significantly to the stability of the electron pair on C_1 . For benzyl, one can see that the electron pair is somewhat localized on the substituent by comparing its electron affinity with that of heptatrienide ($EA(CH_2(CH)_5CH_2) = 1.27 \pm 0.03$ eV) [31], which has a fully conjugated π system to which the electron pair contributes. But the ring still stabilizes the lone pair, as can be seen by comparing with the electron affinities of alkanes that contain no conjugated systems; for instance, $EA(CH_3CH_2) = -0.26 \pm 0.11$ eV [32] and $EA(CH_3CH_2CH_2) = -0.07 \pm 0.22$ [32]. In phenoxyl, the higher electron affinity of the oxygen atom (1.4 eV), combined with the stabilization from the ring system, gives the phenoxyl radical an EA of 2.253 eV, more than twice that of benzyl. We can contrast this with the EAs of other oxygen-centered radicals: CH_3O (1.57 ± 0.02 eV) [33], CH_3CH_2O (1.726 ± 0.033 eV) [34], and linear $CH_3(CH_2)_5O$ (1.9 ± 0.2 eV) [35]. While all are higher than those of alkanes, none is close to that of phenoxyl. Thus, even with a highly electron-withdrawing substituent, the aromatic ring is very effective in stabilizing the negative charge in these systems.

One factor we may extract from the geometry calculations on benzyl and phenoxyl is the degree to which the unpaired electrons contribute to the ring aromaticity in the radicals. Examining the phenoxyl radical and anion geometries in Fig. 5, we see from the ring C–C bond length change and the ring C–C–C angles that the π lone pair in the anion changes the ring structure, but in the radical the ring is an essentially unperturbed benzene molecule. Benzyl, however, contains a distorted ring system in both the radical and the anion. Both the phenoxide C–O and the benzyl C–CH₂ bonds are considerably shorter in the anions than in the radicals, showing that some dative double bonding character may be present. However, losing an electron from the anion to the radical has a greater effect on this bond in phenoxide than in benzyl. The C–O bond becomes an almost pure single bond, while the C–CH₂ bond keeps some double bond character as the unpaired electron has some resonance stabilization.

The reduced participation of the phenoxyl oxygen atom in the ring structure is also evidenced by a comparison [28] of the first excited state energy of the benzyl radical (2.73 eV) with the second excited state energy of the phenoxyl radical (2.3 eV). These transitions are analogous to one another; they correspond to the transfer of an electron from the ring to the substituent, changing the unpaired electron on the substituent, which could delocalize into

the aromatic system, to a lone pair of electrons. The lower value in phenoxyl for this transition indicates that such a change is less costly than in benzyl since the C–O bond cannot lose as much conjugated character as the C–CH₂ bond can.

Angular distributions

The asymmetry parameter β provides information about the orbitals from which electrons are detached. This information is most direct in the case of photodetachment from atoms: since the selection rule for photodetachment is $\Delta l = \pm 1$, electrons coming from s orbitals show p-wave detachment ($\beta \approx 2$), while p orbital electrons can have s-wave or d-wave character. The value of β for detachment from p orbitals depends on photon energy, according to the relative contributions of s and d waves. At threshold the electrons have purely s-wave properties ($\beta = 0$). With an increase in photon energy to 1–2 eV above threshold the electrons approach a $\sin^2 \theta$ distribution ($\beta = -1$), and further increases in photon energy allow d-wave behavior to dominate and a $\cos^2 \theta$ distribution results.

Molecular photodetachment is somewhat more complicated, and β will generally be more isotropic, that is, closer to zero. Work in our laboratory has shown that electrons detached from molecules in the 0–3 eV electron kinetic energy range can be described roughly as s-like if $\beta > 0$, or p-like if $\beta < 0$. Electrons which are s-like generally come from molecular orbitals with fewer nodes or greater symmetry than those which give rise to p-like electrons.

For instance, β is between 0.15 and 0.30 for the peaks in the photoelectron spectrum of phenide. The consistently positive values over the entire progression indicate that the orbital from which the electron is being detached has some s-like character. A simple picture of this molecular orbital would be a nodeless lobe with A₁ symmetry on C₁ and in the plane of the molecule. However, $\beta = -0.42 \pm 0.20$ for the benzyl spectrum, and $\beta = -0.53 \pm 0.20$ for phenoxide. The electron shows more p-like behavior because it is coming from an out-of-plane p orbital on the substituent (–CH₂ or –O), which has B₁ symmetry and has a node in the plane of the molecule.

Thermochemistry

The gas-phase acidities of the protonated analogues of these anions can easily be calculated using the thermochemical cycle:

$$\Delta H_{\text{acid}}(\text{H-A}) = \text{BDE}(\text{HA}) - \text{EA}(\text{A}^-) + \text{IP}(\text{H}) \quad (2)$$

where A is the species in question, BDE(HA) is the bond dissociation energy of the acidic hydrogen, and IP(H) is the ionization potential of the hydrogen

atom. In these experiments, electron affinities can be determined to an accuracy of 6 meV ($0.14 \text{ kcal mol}^{-1}$) [25] while uncertainties in determinations of gas-phase acidities and bond dissociation energies are much larger. Therefore our electron affinity measurements provide an important check of previously determined thermodynamic quantities. The acidities and bond dissociation energies of benzene, toluene and phenol have been measured previously, so that we can close the thermochemical cycle, providing this consistency check and improving the accuracy of these measurements for all three molecules.

Using the bond dissociation energy provided by McMillen and Golden [7] ($110.9 \pm 2 \text{ kcal mol}^{-1}$) and our electron affinity, eqn. (2) gives $\Delta H_{\text{acid}}^{\circ}(\text{C}_6\text{H}_5\text{-H}) = 399 \pm 2 \text{ kcal mol}^{-1}$, which compares favorably to Meot-Ner and Sieck's result [8], $400.8 \pm 2.5 \text{ kcal mol}^{-1}$, as well as the $399 \pm 2 \text{ kcal mol}^{-1}$ reported by DePuy et al. [6]. Using our benzyl electron affinity with the $\text{BDE}(\text{C}_6\text{H}_5\text{CH}_2\text{-H}) = 87.9 \pm 1.5 \text{ kcal mol}^{-1}$ obtained by metathesis reactions with hydrogen iodide [36], we find that $\Delta H_{\text{acid}}^{\circ}(\text{C}_6\text{H}_5\text{CH}_2\text{-H})$ is $380.5 \pm 1.5 \text{ kcal mol}^{-1}$, which agrees with the value reported by Bartmess et al. [37] of $381 \pm 2 \text{ kcal mol}^{-1}$. By combining our phenoxyl EA with the $\text{BDE}(\text{C}_6\text{H}_5\text{O-H}) = 86.5 \pm 2 \text{ kcal mol}^{-1}$ [38], $\Delta H_{\text{acid}}^{\circ}(\text{C}_6\text{H}_5\text{O-H})$ is $348.5 \pm 2 \text{ kcal mol}^{-1}$, in excellent agreement with the previously reported value of $349 \pm 2 \text{ kcal mol}^{-1}$ [39].

CONCLUSION

The electron affinities of phenyl, benzyl and phenoxyl radicals have been determined using photoelectron spectroscopy. Two vibrational frequencies in each of the radicals are observed in the spectra, and these are used in conjunction with ab initio calculations to estimate geometry changes and identify normal coordinates of the active vibrational modes. Asymmetry parameters have been determined for each of the three molecules. Substituent effects on the electron affinities have been explored to help elucidate the extent to which the aromatic ring alters the properties of the substituents. The electron affinities have been used in thermochemical cycles to improve gas phase acidities and homolytic bond dissociation energies.

ACKNOWLEDGMENTS

This work was supported by National Science Foundation Grants No. PHY90-12244 and CHE88-19444. The computers used for the ab initio calculations were funded by National Science Foundation Grant No. CHE90-22151. The authors thank Professors J. Michl and G.B. Ellison for the use of GAUSSIAN programs, as well as Professor C.H. DePuy and Dr. V.M. Bierbaum for helpful discussions.

NOTE ADDED IN PROOF

Since submitting this paper we have become aware of CI quantum chemical calculations by Negri et al. (J. Chem. Phys., 93 (1990) 600) of the structures and normal modes of the ground and first two excited states of the h7- and d7-benzyl radicals. Although their calculations are at a higher level of theory than ours, they do not affect the interpretations presented in this paper.

REFERENCES

- 1 K.M. Ervin and W.C. Lineberger, in N.G. Adams and L.M. Babcock (Eds.), *Advances in Gas Phase Ion Chemistry*, Vol. 1, JAI Press, Greenwich, CT, 1991.
- 2 K.M. Ervin, J. Ho and W.C. Lineberger, *J. Chem. Phys.*, 91 (1989) 5974.
- 3 M.K. Gilles, K.M. Ervin and W.C. Lineberger, *J. Am. Chem. Soc.*, in press.
- 4 D.G. Leopold, A.E. Stevens-Miller and W.C. Lineberger, *J. Am. Chem. Soc.*, 108 (1986) 1379.
- 5 M.J. Frisch, M. Head-Gordon, H.B. Schlegel, K. Raghavachari, J.S. Binkley, C. Gonzalez, D.J. DeFrees, D.J. Fox, R.A. Whiteside, R. Seeger, C.F. Melius, J. Baker, R.L. Martin, L.R. Kahn, J.J.P. Stewart, E.M. Fluder, S. Topiol and J.A. Pople, *GAUSSIAN 88*, Gaussian, Inc., Pittsburgh, PA, 1988.
- 6 C.H. DePuy, V.M. Bierbaum and R. Damrauer, *J. Am. Chem. Soc.*, 106 (1984) 4051.
- 7 D.F. McMillen and D.M. Golden, *Ann. Rev. Phys. Chem.*, 33 (1982) 493.
- 8 M. Meot-Ner (Mautner) and L.W. Sieck, *J. Phys. Chem.*, 90 (1986) 6687.
- 9 R.P. Johnson, *J. Org. Chem.*, 49 (1984) 4857.
- 10 J. Pacansky and D.W. Brown, *J. Phys. Chem.*, 87 (1983) 1553.
- 11 J. Pacansky and J. Bargon, *J. Am. Chem. Soc.*, 97 (1975) 6896.
- 12 M.E. Jacox, *J. Phys. Chem.*, 86 (1982) 670.
- 13 M.J.S. Dewar, W.C. Gardiner, Jr., M. Frenklach and I. Oref, *J. Am. Chem. Soc.*, 109 (1987) 4456.
- 14 G. Vanermen, S. Toppet, M. Van Beylen and P. Geerlings, *J. Chem. Soc., Perkin Trans. 2*, 5 (1986) 699.
- 15 J.H. Miller and L. Andrews, *J. Mol. Spectrosc.*, 90 (1981) 20.
- 16 R.V. Lloyd and D.E. Wood, *J. Chem. Phys.*, 60 (1974) 2684.
- 17 L. Andrews, J.H. Miller and B.W. Keelan, *Chem. Phys. Lett.*, 71 (1980) 207.
- 18 C. Cossart-Magos and S. Leach, *J. Chem. Phys.*, 56 (1972) 1534.
- 19 C. Cossart-Magos and S. Leach, *J. Chem. Phys.*, 64 (1976) 4006.
- 20 P.S. Drzaic and J.I. Brauman, *J. Phys. Chem.*, 88 (1984) 5285.
- 21 Y.A. Kruglyak and E.V. Mozdor, *Theor. Chim. Acta*, 15 (1969) 365.
- 22 B. Ward, *Spectrochim. Acta, Part A*, 24 (1968) 813.
- 23 S.M. Beck and L.E. Brus, *J. Am. Chem. Soc.*, 104 (1982) 1805.
- 24 D.G. Leopold, K.K. Murray, A.E. Stevens-Miller and W.C. Lineberger, *J. Chem. Phys.*, 83 (1985) 4849.
- 25 C.S. Feigerle, Ph.D. Thesis, University of Colorado, 1983.
- 26 M.W. Chase, Jr., C.A. Davies, J.R. Downey, Jr., D.J. Frurip, R.A. McDonald and A.N. Syverud, *J. Phys. Chem. Ref. Data*, 14 (suppl. 1) (1985).
- 27 M.E. Jacox, *J. Phys. Chem. Ref. Data*, 19 (1990) 1500.
- 28 H.M. Chang and H.H. Jaffe, *Chem. Phys. Lett.*, 23(1) (1973) 146.
- 29 (a) J. Cooper and R.N. Zare, *J. Chem. Phys.*, 48 (1968) 942.

- (b) J. Cooper and R.N. Zare, *J. Chem. Phys.*, 49 (1968) 4252.
(c) J.L. Hall and M.W. Siegel, *J. Chem. Phys.*, 48 (1968) 943.
- 30 J. Pacansky, G.P. Gardini and J. Bargon, *J. Am. Chem. Soc.*, 98 (1976) 2665.
31 A.H. Zimmerman, R. Gygax and J.I. Brauman, *J. Am. Chem. Soc.*, 100 (1978) 5595.
32 C.H. DePuy, S. Gronert, S.E. Barlow, V.M. Bierbaum and R. Damrauer, *J. Am. Chem. Soc.*, 111 (1989) 1968.
33 P.C. Engelking, G.B. Ellison and W.C. Lineberger, *J. Chem. Phys.*, 69 (1978) 1826.
34 G.B. Ellison, P.C. Engelking and W.C. Lineberger, *J. Phys. Chem.*, 86 (1982) 4873.
35 S.G. Lias, J.E. Bartmess, J.F. Liebman, J.L. Holmes, R.D. Levin and W.G. Mallard, *J. Phys. Chem. Ref. Data*, 17 (suppl. 1) (1988).
36 M.J. Rossi and D.M. Golden, *J. Am. Chem. Soc.*, 101 (1979) 1230.
37 J.E. Bartmess, J.A. Scott and R.T. McIver, Jr., *J. Am. Chem. Soc.*, 101 (1979) 6047.
38 F.G. Bordwell, J.-P. Cheng and J.A. Harrelson, Jr., *J. Am. Chem. Soc.*, 110 (1988) 1229.
39 M. Fujio, R.T. McIver, Jr. and R.W. Taft, *J. Am. Chem. Soc.*, 103 (1981) 4017.